



Anatomical, behavioural, and histopathological evaluation of colostrum in streptozotocin-induced diabetic retinopathy in Swiss albino mice

Aswinprakash Subramanian^{1,2}, JayaramanThirunavukkarasu^{2,*}, Arunachalam Muthuraman^{3,*}

¹Anatomy Unit, Faculty of Medicine, AIMST University, 08100 Bedong, Kedah, Malaysia.

²Dept of Pharmacology, Saveetha Institute of Medical & Technical Sciences (SIMATS), Saveetha University, Chennai-602105, Tamilnadu, India.

³Pharmacology Unit, Faculty of Pharmacy, AIMST University, 08100 Bedong, Kedah, Malaysia.

*Corresponding author : Dr. Arunachalam Muthuraman
Unit of Pharmacology, Faculty of Pharmacy,
AIMST University, Semeling, 08100 Bedong,
Kedah DarulAman, Malaysia.

Abstract

Diabetic retinopathy (DR) is the most common and leading cause of diabetic ocular complications. The progression of DR is alleviating the quality of life. The chronic conditions make diabetes-associated macro/microvascular complications. The prevalence rate is higher about 17.4/1000 persons every year. The available medicines for attenuation of DR are limited. Colostrum (CLS) is obtained from a natural source. It is reported to prevent various chronic disorders like diabetes, cardiac disease, and blood pressure. However, the effect of CLS remains to be elusive for the management of DR. Current study was designed to investigate the CLS in DR-associated microanatomical, neurobehavioural, and biochemical changes. DR was induced by administration of streptozotocin (STZ, 35 mg/kg:intraperitoneal; and 20 µl of STZ: intravitreal) in mice. The test compounds *i.e.*, CLS (125 and 250 mg/kg) were administered orally (*p.o.*) for 21 days, after intravitrealinjection of STZ (day 7).The DR-associated neurobehavioural changes *i.e.*, optokinetic motor response (OMR) test, Penta-maze (PM) test, and T-Maze (TM) tests were assessed in different time intervals. Further, biomarkers *i.e.*, blood glucose; retinal tissue thiobarbituric acid reactive substances (TBARS), and reduced glutathione (GSH)were estimated. The reference drug *i.e.*, dexamethasone (DEX, 10 mg/kg; *p.o.*) was administered for 21 consecutive days. The administrations of CLS were shown to ameliorate the DR-associated microanatomical, neurobehavioural, and biochemical changes. These results were similar to DEX treated group. Hence, CLS can be used as a natural medicine for the management of DR due to its potential antioxidant, anti-inflammatory, neuroendocrine, and neurochemical actions.



Keywords:Intravitreal injection;neuroendocrine function;neurovascular complication;optokinetic motor response; retinal degeneration; visual function.

DOI Number: 10.14704/nq.2022.20.8.NQ44363

NeuroQuantology 2022; 20(8): 3332-3347

Introduction

Diabetes mellitus is a metabolic disorder and it elevates the blood sugar levels via damage of pancreatic beta cells (Insulin secreting cells) and the development of resistance of insulin receptors. The progression of diabetes mellites is occurred mainly due to the changes of lifestyle changes. In chronic conditions, the quality of life is also altered with diabetes mellitus via the generation of secondary complications. The major secondary complications are diabetic cardiomyopathy, diabetic nephropathy, diabetic neuropathy, and diabetic retinopathy (DR) (Nellaiappan et al., 2021). These complications mainly occur with advanced glycation end products (AGE) lead to cause cellular oxidant stress, inflammation (lipid peroxidation), mitochondrial dysfunction, alteration of ion channel states, and functional changes of deoxyribonucleic acid (DNA) & messenger ribonucleic acid (mRNA) (Gora et al., 2021).

These cellular and molecular alterations also affect the vascular systems, cholesterol regulations, barrier functions, and metabolic enzymes leading to worsening conditions of the degree of heart attack, rheumatoid arthritis, osteoporosis,stroke, and the aging process. Anatomically, these secondary complications are categorized as macro/microvascular complications(Mota et al., 2020). DR is a microvascular complication of diabetes mellites. The incidence rate of DR is higher *i.e.*, 17.4/1000 persons/year (Williams et al., 2004). The level of DR is categorized based on the degree of variations like microaneurysms, hemorrhages, hard exudates, cotton wool spots, venous changes, new vessel formation, and macula thickening (Wang et al., 2020). The treatment of DR is remained a challenge due to the involvement of too complex mechanisms.

Some of the drugs manage the severity of DR progressions like dexamethasone and intravitreal triamcinolone(Hong et al., 2020; Kuley et al., 2020). The chronic administration of these agents has shown multiple adverse effects like endophthalmitis, intraocular inflammation, increase intraocular tension (IOT), and ocular hemorrhage (Chatziralli, 2021).

The various animal models are employed for the screening of newer medicines for the management of retinopathy. Diabetes mellites are induced experimental animals very commonly made with the administration of alloxan, streptozotocin (STZ), hyperoxia, Intravitreal toxin (pro-inflammatory cytokines&hydrogen peroxide, and N-methyl-D-aspartate), surgical pancreatectomy, and spontaneous diabetes with genetic manipulation. Besides, these models are also known to cause secondary complications,especially DR(Gómez-Vicente et al., 2015; Huang et al., 2018; Mugisho et al., 2018; Robinson et al., 2012). Even, the DR is accelerated by intravitreal (*i.vit.*) injection of STZ and it is inducing retinal inflammation and neuronal degeneration in Lewis rats(Kermorvant-Duchemin et al., 2013).

CLS is a nutrient-rich fluid of female mammals. It is also known as first milk, secretes after giving birth. It has potential ingredients for boosting the immune system, body growth, and factors for tissue repairs. The presences of large quantities of complement components support to produce the natural anti-microbial actions via stimulation of the immune system (Mishra, 2020). Besides, the preparation of bovine colostrum is also used to treat infections in the gastrointestinal system (Sienkiewicz et al., 2021). Further, it enhances the growth of the body and repairs the damaged tissue to the presence of growth factors *i.e.*, transforming growth factors alpha & beta (TGF- α & TGF- β);

3333



and insulin-like growth factors 1 & 2 (Uruakpa et al., 2002). However, the role of CLS in DT remains to be explored. Hence, the present study is designed to explore the role of CLS in the accelerated DR model with the assessment of anatomical, visual behavioral, and histopathological observations.

Materials and methods

Animal

The disease-free Swiss albino mice (12 months old; 20-30 g) were used in this research work. Animals were maintained in the central animal house, AIMST University with a standard laboratory diet (Soon-Soon Oilmills Sdn Bhd, Pinang, Malaysia). The animal was allowed to access the free water *ad libitum*. The 12 hours of natural light and dark cycles were maintained. The macro-environmental temperature and humidity of animal houses were made at 25 °C and 50%. The experimental protocol was approved by AIMST University Animal Ethics (AUAEC/FOM 2020/21 – Amendment No. 1). The care of animals was taken as per the guidelines of AUAEC).

Induction of diabetic retinopathy (DR)

Diabetic Mellitus was induced by the administration of streptozotocin (STZ) as described by Yuan *et al.* (2014) and Tawfik *et al.* (2019). The DR was developed by a single intraperitoneal injection of streptozotocin (STZ; 35 mg/kg). The acceleration of retinopathy was made on the 7th day of diabetic mice by intravitreal (*i.vit.*) injection of STZ (20 µl of 7 % w/v of STZ stock solution).

Experimental protocol

Seven groups of male adult mice (n = 8) were employed in this study. Group-I served as a normal control group. Group II served as the diabetic retinopathy (DR) group. Diabetes was induced by intraperitoneal (*i.p.*) administration of STZ (35 mg/kg) and it is considered day 1. Day 3 was confirmed diabetic condition with blood glucose estimation. The progression of retinopathy was accelerated by intravitreal

(*i.vit.*) administration of 20 µl of 7 % w/v STZ stock solution on day 7. Group III and IV served as test compound treatment groups *i.e.*, colostrum (CLS) doses of 125 and 250 mg/kg; oral administration for 21 consecutive days respectively (from day 8). Group V served as a reference drug treatment group *i.e.*, dexamethasone (DEX), 10 mg/kg; oral administration for 21 consecutive days (from day 8).

The blood glucose level was estimated on day 3 and day 21. The body weight was assessed on day 8 and day 28. The behavioral responses *i.e.*, optomotor response (OMR; 7, 14, 21, and 28th days), Penta-maze (PM; 7, 14, 21, and 28th days), and T-Maze (TM21 and 28th days) were assessed on different time intervals *i.e.*, 7, 14, 21 and 28th days. The molecular mechanisms were confirmed by estimation of retinal tissue thiobarbituric acid reactive substances (TBARS), reduced glutathione (GSH), and aldose reductase (AR) activities. The micro-anatomical changes were analyzed by histopathological observation of mice's retinal tissue.

Analysis of gross anatomical changes

The changes in mice eyeball gross anatomy was analyzed as described method by Schnichel *et al.* (2020). The mice's eyeballs were harvested on day 28 after the assessment of behavioral observations. The eyeballs were placed on a transparent graph sheet (a graph 1x1 mm square was printed overhead projector sheet). The development of opacities with DR and other groups was observed. Besides, the axial length (as a diameter) was also assessed with a transparent graph sheet using a stereomicroscope. The retinal colour, the ratio of eye/body weight, and water content were also analyzed.

Analysis of mice retinal micro-anatomical changes

The mice's eyeballs were harvested on day 28 after the assessment of behavioral observations. The eyeball tissues were fixed



with neutral buffered 10% paraformaldehyde solution. The tissue block was prepared with paraffin wax. The embedded mice eyeball tissue blocks were used for the sagittal sectioning under the semi-automatic cryo-microtome device. The 5 μm sectioned tissues were used for the further process of Hematoxylin-Eosin (H & E) staining. The stained slides were observed for micro-anatomical changes in the retinal layers of mice eyeballs under 400x magnification. The changes were noted and compared with normal and reference control animal tissue sections. Normally, ganglionic layers of rods and cones (in the retina) in mice are arranged without any abnormalities like vacuolations, retinal detachment, and proliferation of blood vessels.

Assessment of DR-associated behavioural changes

The DR-associated visual behavioral changes were assessed at different time intervals *i.e.*, OMR and PM tests were carried out on the 7, 14, 21, and 28th days of experimental protocol for assessing the visual acuity responses. The TM test was performed on the 21st and 28th days of the experimental protocol for the assessment of acute visual cognitive functions.

Assessment of visual acuity functions by OMR test device

The optokinetic motor response (OMR) was used for the assessment of DR-associated visual impairments. The OMR was carried out as described method by Prusky *et al.* (2004) with a slight modification of Kretschmer *et al.* (2015). Briefly, the OMR device consists of two concentric circular chambers. It is covered with a non-transparent square box (inner side dark environment created). The white light-emitting diode (LED) strip light was placed on the inner wall of the square box. The inner wall of the big circular chambers is made with multiple black and light stripes and positioned vertically. This is connected to a 10-rpm motor to make a rotating drum. The non-revolving smaller

transparent circular chamber was placed at the center of the OMR device. Mice were placed in this smaller chamber. In this condition, mice can see the outer black and light strip movements. The visual acuity test was assessed based on the responses of the animal movement against the clockwise and counter-clockwise movements of the outer (transparent circular) chamber. The recorded animal movements were observed *i.e.*, no of rearing within the 4 minutes observation period. The assessments were repeated three times to get reproducible data with OMR responses.

Assessment of spatial imagery transformation functions by PM test device

The mice visual function test was assessed by using the 'Penta-maze' test device as a described method by Rondi-Reiget *et al.* (2006) with minor modification of Vorhees and Williams (2014). Briefly, it is like a star-shaped maze device. PM device is built with poly-acrylic materials. It is a circular shape and consists of five-way water channels with solid central pentagon objects. These five waterway channels are radiated equally from the pentagon center. The walls of the PM device are made in uniform colour and filled with water. And, the water was made opaque with non-toxic dye. The one arm of the PM device is always considered as starting point. Further, it was made with two pathways *i.e.*, allocentric (object-to-object representation) and egocentric (self-to-object representation) to enter differential destination points. These destination points were cued with red and green LED illumination with a platform. Each pathway wall was made with unique imaginary cues. The analysis of allocentric navigation was made by mice reaching the individual destination point (called absolute location *i.e.*, submerged platform) via particular pathways, whereas the presence of available extra wall cues in alternative pathways. The allocentric navigation training was given on the 22nd day of the experimental protocol. On the 23rd day, an egocentric response was made by placing the



animal nearest arm of the destination points of the PM device (platform available in destination and starting points). During egocentric response recording, the wall navigation cues are removed and the individual destination point platform was made as a visible condition. Thereafter, the egocentric response was recorded as the percentage preference of mice reaching the destination point (PR) with the use of the same learned route during allocentric training and without the concern of absolute location cues within the 5 minutes observation period. The strategies of spatial imagery transformation functions are described by Fouquet *et al.* (2013).

Assessment of visual exploratory behaviour by TM test device

The rodent TM device was used for the assessment of various neuro-behavioral patterns like anxiety; learning & memory functions; and spontaneous alternation with minor modification and assessment patterns. The spontaneous alternation test in TM is used for the assessment of the exploratory behavior of rodents. The visual exploratory behavior (alternation) of mice was assessed by using the TM test device as a described method by Deacon and Rawlins (2006). Briefly, the TM alternation test device consists of an arm's length of 30 cm; width of 10 cm; enclosed wall height of 20 cm; and an extended central portion has 7 cm of partition. On the 22nd day, the animal was placed on the starting point of the TM device. Animals are allowed to choose their entry on either left or right side of the TM arm. The right arm considers to goal-directed arm with food placement. The trials were standardized with normal animals. The repeated trials were performed until the normal animal visual exploratory behavior shows a lower tendency to enter a last visited arm. Similar numbers of trials were applied in all the groups of animals. On the 23rd day, the mouse's visual exploratory behavior is assessed as the percentage alternation (PA) with an indication of the number of turns to the goal-directed arm

(right) side within the 5 minutes observation period.

Biochemical estimations

On the 28th day, all the animals were anesthetized with diethyl ether. The blood drops were collected via the tail vein puncture method and blood glucose was estimated by using a commercial Accu-Chek glucometer device. Thereafter, animals were sacrificed, and retinal and brain tissues were collected for the estimation of tissue biomarker changes like TBARS, GSH, AR, and total protein levels. The details of all biomarker estimations are explained in the following sections.

Estimation of TBARS as an indication of lipid peroxidation

The retinal tissue TBARS level was estimated as a described method by Ohkawa *et al.* (1979). Briefly, 0.2 ml of supernatant of homogenate was mixed with 0.2 ml of 8.1 % sodium; 0.2 ml of 8.1 % sodium dodecyl sulphate; 1.5 ml of 30 % acetic acid; and 1.5 ml of 0.8 % of thiobarbituric acid (TBA) in a test tube. The total volume was made up to 4 ml with distilled water. Further, test tubes were incubated at 90 °C for 1 hour. Then, 1 ml of distilled water was added and centrifuged for 10 minutes at 4000 revolutions per minute (rpm). The pink colour chromogen was developed. The changes in absorbance of pink colour chromogen were recorded by using a spectrophotometer (DU 640B Spectrophotometer, Beckman Coulter Inc., CA, USA) at 532nm. The standard curve was prepared reference standard *i.e.*, 0-100 nanomole of 1,1,3,3-tetra methoxy propane (TMP) per milliliter. The net value of MDA was expressed as nmol of MDA per mg of protein.

Estimation of GSH as an indication of oxidative stress

The retinal tissue GSH level was estimated as a described method by Ellman (1959). Briefly, the retinal tissue supernatant was mixed with 10% w/v of trichloroacetic acid



(1:1 ratio) to make the protein precipitations. Then, test tube samples were centrifuged at 1000 rpm for 10 min at 4 °C. About 0.5 ml of clear aliquot was mixed with 2 ml of 0.3 M disodium hydrogen phosphate. Thereafter, 0.25 ml of 0.001 M freshly prepared 5,5'-dithiobis (2-nitrobenzoic acid) (DTNB) solution was added. The DTNB was dissolved in 1% w/v sodium citrate solution. The yellow colour chromogen was developed. The changes in absorbance of yellow colour chromogen were recorded by using a spectrophotometer (DU 640B Spectrophotometer, Beckman Coulter Inc., CA, USA) at 412nm. The standard curve was prepared with reference standard *i.e.*, 10-100 micromole of GSH per milliliter. The net value of GSH was expressed as μmol of GSH per mg of protein.

Estimation of AR as an indication of activation of polyol pathways

$$\text{AR activity} = \frac{\delta \text{ O. D. normal control sample} - \delta \text{ O. D. disease or treatment samples}}{\delta \text{ O. D. of the normal control sample}}$$

In this formula, 'δ O.D.' represents the changes in absorbance/minutes. The AR activity was noted corresponding to the production of $1\mu\text{M}$ of NADP^+ from NADPH per 1 min. The net value of AR was expressed as a unit per minute per mg of protein (U/min/mg of protein).

Estimation of total proteins

The retinal and brain tissue total protein level was estimated as a described method by Lowry *et al.* (1951). Briefly, the 0.15 ml of tissue supernatant was diluted up to 1 ml with phosphate buffer. Then, 5 ml of Lowry's reagent was added to all the test tubes. Lowry's reagent consists of two major reaction mixtures *i.e.*, 1) Reagent A: It consists of 2 grams of sodium potassium tartrate; 100 grams of sodium carbonate; and 500 ml of 1N sodium hydroxide in one liter of distilled water. 2) Reagent B: It consists of 2 grams of sodium potassium tartrate; 1 gram of copper sulfate; 90 ml of distilled water; and 10 ml of 1N sodium hydroxide. Reagents A and B were mixed 9:1

The retinal AR activity levels were estimated as a described method by Guest (2019) with a slight modification of Hayman and Kinoshita (1965). Briefly, 300 μl of tissue homogenate was mixed with 2700 μl of assay buffer with a ratio of 1:9 respectively. The assay buffer (pH 6.2) consists of 50 mmol/L of phosphate; 400 mmol/L of lithium sulphate (Li_2SO_4); 10 mmol/L of DL-glyceraldehyde; and 0.1 mmol/L of nicotinamide adenine dinucleotide phosphate (NADPH). The subtract blank consisted of a 3ml assay buffer reflecting NADPH oxidation in the absence of enzyme (tissue homogenate) samples. The changes in absorbance were recorded at 0, 5, 10, and 15 minutes by using a spectrophotometer (DU 640B Spectrophotometer, Beckman Coulter Inc., CA, USA) at 340 nm. The level of AR activity was quantified by using the following formula.

ratio respectively. This reagent is called Lowry's reagent and uses total protein estimation. The sample and Lowry reagent containing test tubes were mixed thoroughly and allowed to stand for 15 min at room temperature. Thereafter, 0.5 ml of Folin-Ciocalteu reagent (10 grams of sodium tungstate and 2.5 grams of sodium molybdate are dissolved in 70 ml of distilled water; further 5 ml of 85% phosphoric acid and 10 ml of concentrated hydrochloric acid are added) was added and vortexed vigorously. Then, test tubes were incubated at room temperature for 30 min. The purple colour chromogen was developed. The changes in absorbance of purple colour chromogen were recorded by using a spectrophotometer (DU 640B Spectrophotometer, Beckman Coulter Inc., CA, USA) at 750nm. The standard curve was prepared with 0.2-2.4 milligram of bovine serum albumin (BSA) per milliliter. The total protein level was noted as mg/ml.

Statistical analysis



All the results were expressed as mean \pm standard deviation (SD). The behavioral data were statistically analyzed using two-way analysis of variance (ANOVA) followed by the Bonferroni post hoc test and data of tissue biomarkers *i.e.*, TBARS, GSH, and AR levels were analyzed using one-way ANOVA followed by Tukey's Multiple Range test using Graph pad prism version-5.0 software. The value of $p < 0.05$ was considered to be statistically significant.

Results

Effect of CLS in DR associated gross anatomical changes

The administration of STZ (35 mg/kg; *i.p.*; and 20 μ l of 7 % w/v; *i.vit.*) were showed significant vasculogenesis with enlargement of blood vessels in the retina with hemorrhage. The comparison with CLS (125 and 250 mg/kg; *p.o.*) were showed significant regression of proliferation of blood vessels against the DR-associated eyeball changes. These results were comparable to the reference drug (DEX; 10 mg/kg) treatment. The results of the CLS effect in DR-associated eyeball changes were illustrated in Figure 1.

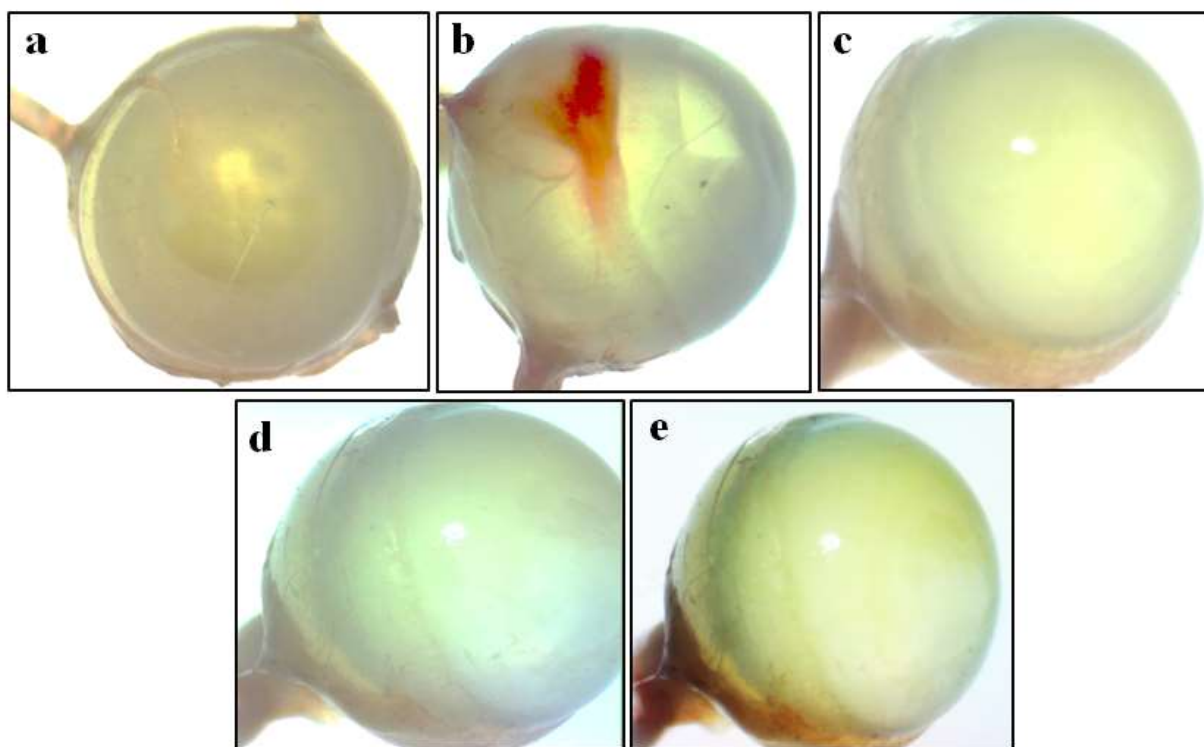


Figure 1. Effect of CLS in DR associated gross anatomical changes. Figure 1a-1e showed gross anatomical changes in normal, DR, AST (10, and 20 mg/kg), and DEX (10 mg/kg) treated groups respectively. Figure 1a showed normal architecture of the retinal layer of mice without any proliferation of blood vessels. Figure 1b showed vasculogenesis with enlargement of blood vessels in the retina with hemorrhage. Figure 1c showed regression of proliferation of blood vessels. Figure 1d showed a significant reversal of DR-associated proliferation of blood vessels. Figure 1e showed potential improvement of retinal layers against the DR.

Effect of CLS in DR-induced retinal micro-anatomical changes

The administration of STZ (35 mg/kg; *i.p.*; and 20 μ l of 7 % w/v; *i.vit.*) was shown potential induction of DR. It showed DR-

associated retinal micro-anatomy changes like enlargement of blood vessels in the inner retina; extravasation of blood into the vitreous region; extensive vacuolations in the inner plexiform layers & a ganglionic layer of the retina; and disarrangement of retinal cell layers when compared to naïve animal group. The administration of CLS (125 and 250 mg/kg; *p.o.*)

attenuates the DR-associated micro-anatomical alteration in the retina of mice dose-dependent manner. The effect of CLS showed a similar ameliorative effect to the administration of reference drug *i.e.*, DEX (10 mg/kg; *p.o.*) treated group. The results were illustrated in Figure 2a-2e.

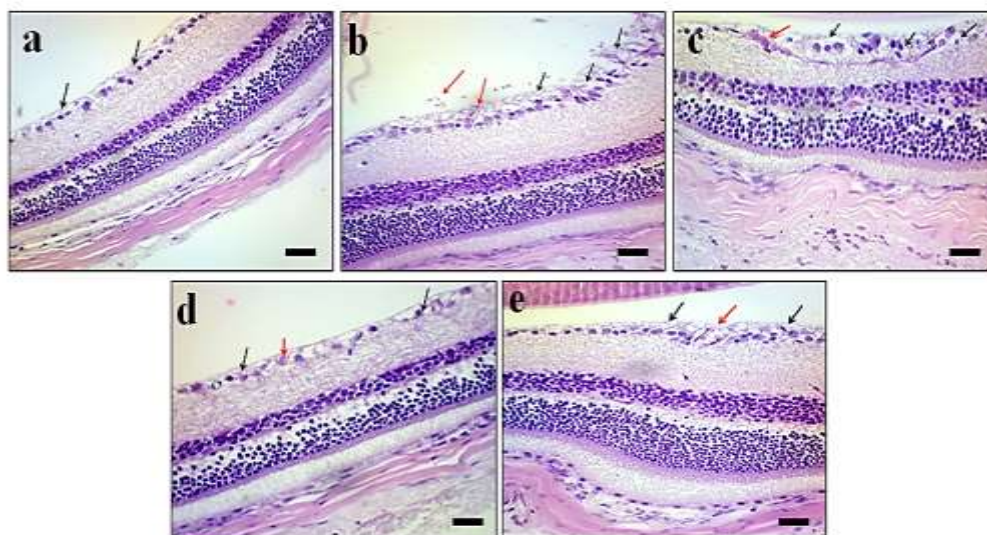


Figure 2. Effect of CLS in DR-induced retinal micro-anatomical changes. Figure 2a-2e showed a histopathological image of sagittal sections of normal mice retinal tissue of normal, DR, CLS (125 and 250 mg/kg), and DEX (10 mg/kg) treated groups respectively. In the figure, a thin arrow shows the arrangement of a retinal layer of a mice's retina. Fig 2a showed the arrangement of a retinal layer of mice retina without any vacuolations and engorgement of blood vessels (black arrow). Fig 2b showed enlarged blood vessels in the inner retina; & extravasation of blood into the vitreous region (red arrow); and disarrangement of retinal cell layers (black arrow). Fig 2c showed a mild reduction in the number & size of enlarged blood vessels in the inner retina region (red arrow); and mild derangement of retinal cell layers (black arrow). Fig 2d showed normal blood vessels appearing in the inner retina region (red arrow); and an orderly arrangement of retinal cell layers (black arrow). Fig 2e showed a reduction in the number & size of enlarged blood vessels & normal blood vessels appearing in the inner retina region (red arrow); and an orderly arrangement of retinal cell layers (black arrow). Figures 2c-2e showed treatment of CLS (125 and 250 mg/kg) and DEX (10 mg/kg) were decrease the DR-induced histopathological changes. Microscopic examinations were performed under 450 × light microscopy, scale bar 35 μm.

Effect of CLS in DR-induced visual behavioural changes

The administration of STZ (35 mg/kg; *i.p.*; and 20 μl of 7 % w/v; *i.vit.*) showed significant ($p < 0.05$) visual behavioral changes along with DR-associated retinal micro-anatomy changes when compared to naïve animal group. The administration of CLS (125

and 250 mg/kg; *p.o.*) ameliorates significantly the visual behavioral changes *i.e.*, OMR, PM, and TM tests dose-dependent manner when compared to the DR group. The effect of CLS is shown a similar effect to the comparison of reference drugs *i.e.*, DEX (10 mg/kg; *p.o.*) treated group. The details of described in the following section.

Effect of CLS in DR-induced OMR test

The administration of STZ (35 mg/kg; *i.p.*; and 20 μ l of 7 % w/v; *i.vit.*) showed significant ($p < 0.05$) impairment of visual acuity functions in the OMR test as an indication of a decrease in the number of rearing when compared to the normal control

group. The administration of CLS (125 and 250 mg/kg; *p.o.*) significantly ameliorates the above OMR test responses when compared to the DR group. These ameliorative effects were shown a similar effect to the reference drug *i.e.*, DEX (10 mg/kg; *p.o.*) treated group. The results were illustrated in Figure 3.

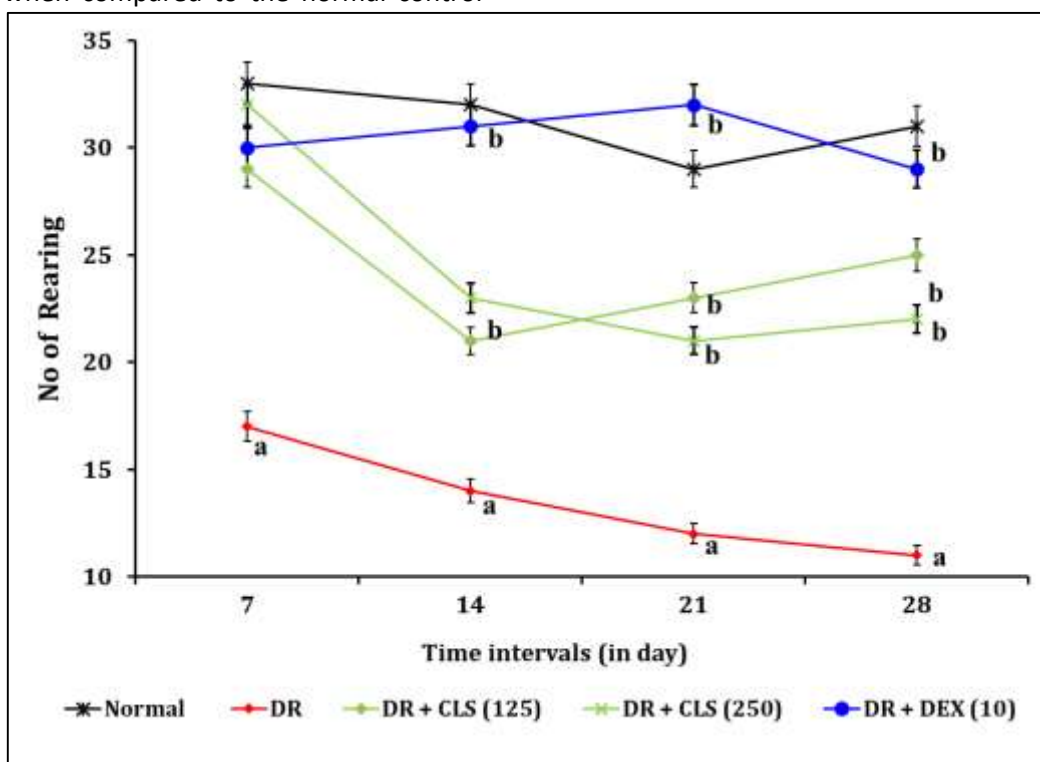


Figure 3. Effect of CLS on DR-induced rearing in OMR test. Digits in parenthesis indicate a dose of mg/kg. Data were expressed as mean \pm SD, $n = 8$ mice per group. ^a $p < 0.05$ Vs normal group; ^b $p < 0.05$ DR group. Abbreviation: CLS, colostrum; DEX, dexamethasone; and DR, diabetic retinopathy.

Effect of CLS in DR-induced PM test

The administration of STZ (35 mg/kg; *i.p.*; and 20 μ l of 7 % w/v; *i.vit.*) showed significant ($p < 0.05$) impairment of spatial imagery transformations in the PM test as an indication of a decrease in the PR value when compared to the normal control group. The

administration of CLS (125 and 250 mg/kg; *p.o.*) significantly ameliorates the PM test responses when compared to the DR group. These ameliorative effects were shown a similar effect to the reference drug *i.e.*, DEX (10 mg/kg; *p.o.*) treated group. The results were illustrated in Figure 4.

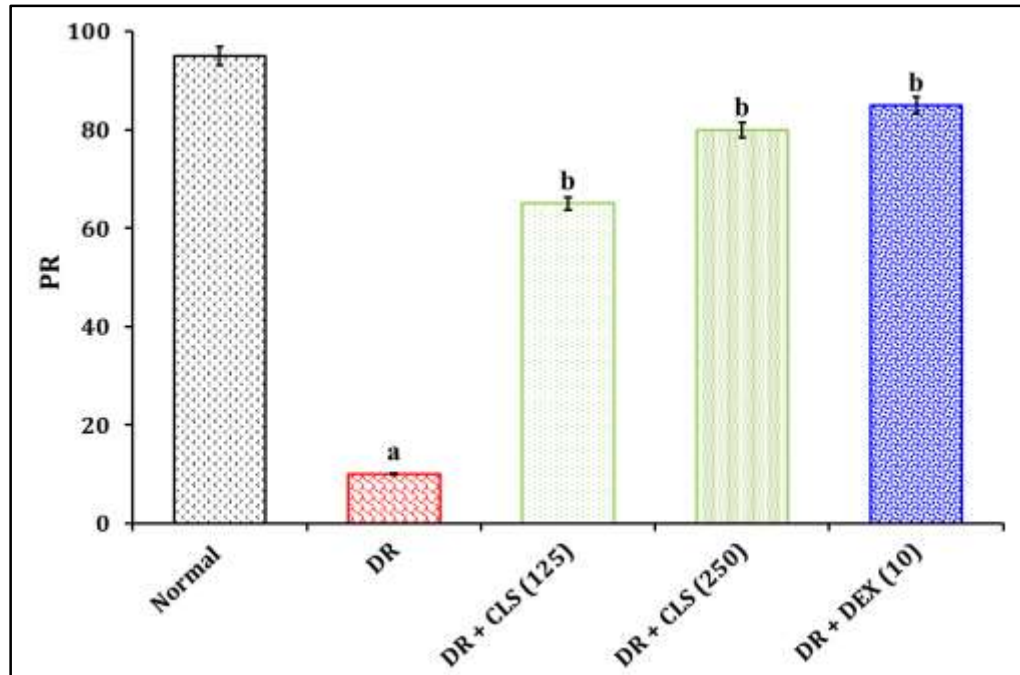


Figure 4. Effect of CLS on DR-induced PR in PM test. Digits in parenthesis indicate a dose of mg/kg. Data were expressed as mean \pm SD, n = 8 mice per group. ^a $p < 0.05$ Vs normal group; ^b $p < 0.05$ DR group. *Abbreviation:* CLS, colostrum; DEX, dexamethasone; DR, diabetic retinopathy; and PR, percentage response to reach the destination point.

3341

Effect of CLS in DR-induced TM test

The administration of STZ (35 mg/kg; *i.p.*; and 20 μ l of 7 % w/v; *i.vit.*) showed significant ($p < 0.05$) impairment of visual exploratory behaviour in the TM test as an indication of a decrease in the P value when compared to the normal control group. The

administration of CLS (125 and 250 mg/kg; *p.o.*) significantly ameliorates the above TM test responses when compared to the DR group. These ameliorative effects were shown a similar effect to the reference drug *i.e.*, DEX (10 mg/kg; *p.o.*) treated group. The results were illustrated in Figure 5.

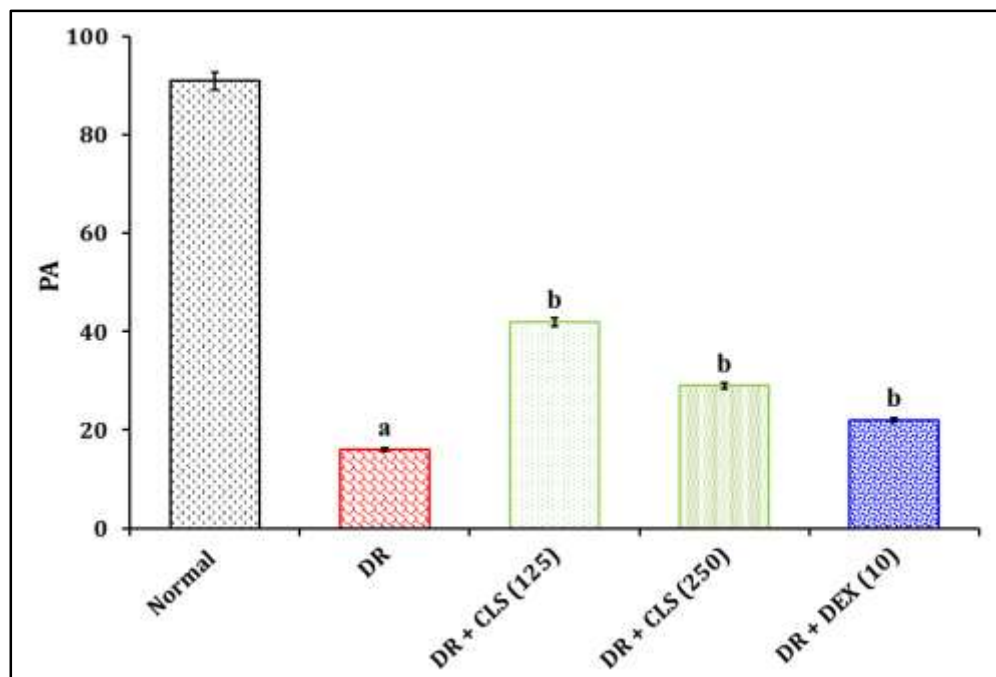


Figure 5. Effect of CLS on DR-induced PA in TM test. Digits in parenthesis indicate a dose of mg/kg. Data were expressed as mean \pm SD, n = 8 mice per group. ^a $p < 0.05$ Vs normal group; ^b $p < 0.05$ DR group. *Abbreviation:* CLS, colostrum; DEX, dexamethasone; DR, diabetic retinopathy; and PR, percentage alternation.

3342

Biochemical estimations

On the 28th day, all the animals were anesthetized with diethyl ether. The blood drops were collected via the tail vein puncture method and blood glucose was estimated by using a commercial Accu-Chek glucometer device. Thereafter, animals were sacrificed and retinal tissues were collected for the estimation of tissue biomarker changes like TBARS, GSH, AR, and total protein levels. The details of all biomarker estimations are explained in the following sections.

Effect of CLS in STZ induced changes in blood glucose level

The administration of STZ (35 mg/kg; *i.p.*; and 20 μ l of 7 % w/v; *i.vit.*) showed a significant ($p < 0.05$) rising in blood glucose level on day 3 and day 28 when compared to the normal control group. It was indicated as the progression of diabetic complications with elevated blood glucose levels. The administration of CLS (125 and 250 mg/kg; *p.o.*) significantly ameliorates the STZ-induced elevated blood glucose level on the 28th day when compared to the DR group. Whereas, the administration of DEX (10 mg/kg; *p.o.*) is partially reduced the STZ-induced elevated blood glucose level. The results were illustrated in figure 6.



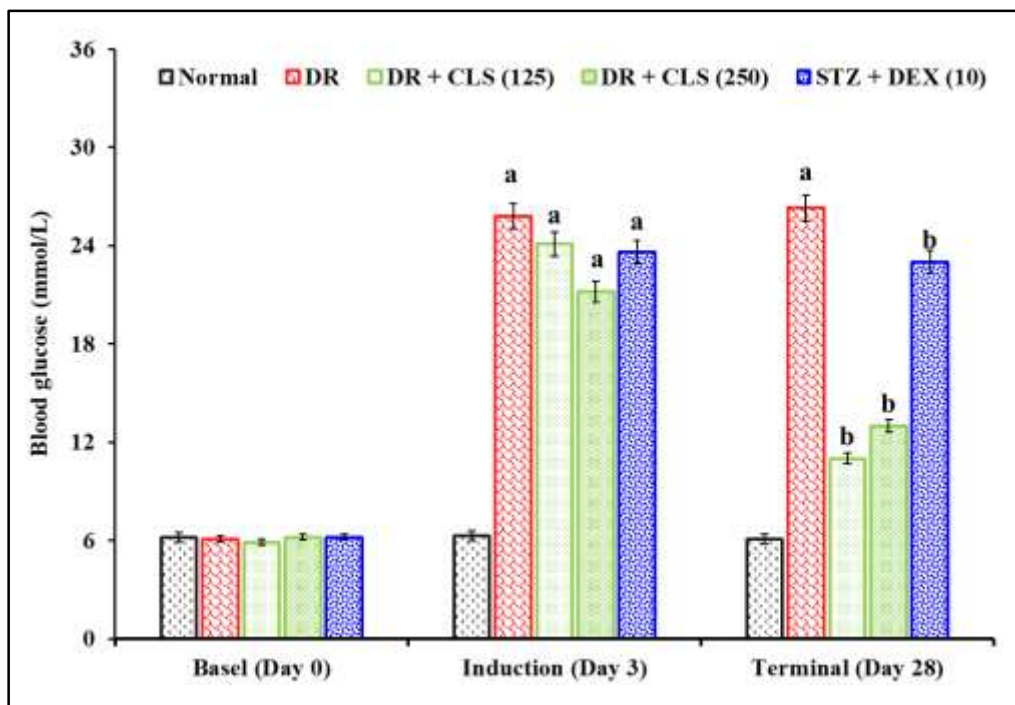


Figure 6. Effect of CLS on STZ-induced changes of blood glucose level. Digits in parenthesis indicate a dose of mg/kg. Data were expressed as mean ± SD, n = 8 mice per group. ^ap < 0.05 Vs normal group; ^bp < 0.05 DR group. *Abbreviation:* CLS, colostrum; DEX, dexamethasone; and DR, diabetic retinopathy.

3343

Effect of CLS in STZ-induced tissue biomarker changes

The administration of STZ (35 mg/kg; *i.p.*; and 20 µl of 7 % w/v; *i.vit.*) were showed significant (*p* < 0.05) alteration of tissue biomarkers when compared to the normal control group. The administration of CLS (125 and 250 mg/kg; *p.o.*) significantly attenuated

the STZ-induced changes in tissue biomarkers when compared to the DR group. It is indicated that CLS has the regulatory role of blood glucose in this experimental model. These ameliorative effects were shown a similar effect to the reference drug *i.e.*, DEX (10 mg/kg; *p.o.*) treated group. The results were indicated in Table 1.

Table 1. Effect of CLS in STZ-induced tissue biomarker changes.

Groups	TBARS (nmol/mg of protein)	GSH (µmol/mg of protein)	AR (U/min/mg of protein)
Normal	1.25 ± 0.024	26.12 ± 1.64	7.52 ± 1.13
DR (35)	3.65 ± 0.078 ^a	7.94 ± 1.32 ^a	19.26 ± 0.91 ^a
DR + CLS (125)	2.01 ± 0.045 ^b	21.74 ± 1.13 ^b	11.08 ± 0.71 ^b



DR + CLS (250)	1.46 ± 0.016 ^b	23.65 ± 1.27 ^b	9.84 ± 1.26 ^b
DR + DEX (10)	1.31 ± 0.082 ^b	25.91 ± 1.04 ^b	8.93 ± 0.78 ^b

Digits in parenthesis indicate dose mg/kg. Data were expressed as mean ± SD, n = 8 mice per group. ^a*p* < 0.5 Vs normal group. ^b*p* < 0.5 Vs DR group. *Abbreviation*: AR, aldose reductase; CLS, colostrum; DEX, dexamethasone; DR, diabetic retinopathy; GSH, reduced glutathione; and TBARS, thiobarbituric acid reactive substances.

Discussion

The administration of STZ (35 mg/kg; *i.p.*; and 20 µl of 7 % w/v; *i.vit.*) shows significant (*p* < 0.05) induction of DR. It is reflected as enlargement of blood vessels, extravasation of blood, extensive vacuolations, and disarrangement of retinal cell layers in the vitreous regions. In addition, DR animal was also shown alterations of visual behavioral changes *i.e.*, OMR (decrease in the number of rearing), PM (decrease the PR), and TM (decrease the PA) tests. Similarly, DR-induced animal tissue biomarkers *i.e.*, TBARS, and AR, increased and decreased the level of GSH. Whereas, the administration of CLS (125 and 250 mg/kg; *p.o.*) ameliorated the DR-associated micro-anatomical changes of the retina, visual behavioral changes, and tissue biomarkers. Similar effects were observed in the reference drug *i.e.*, DEX (10 mg/kg; *p.o.*) treated group.

Based on the above results, it indicates the *i.vit.* injection of STZ-induced modification of retinal microanatomical features. It is clearly expressed *asi.vit.* injection of STZ in diabetic animals can make the prematurity of retinopathy features *i.e.*, retinal apoptosis, retinal inflammation, and retinal degeneration. These results are similar to the previous research report of the Kermorvant-Ducheminet *al.* (2013) study. Moreover, the *i.vit.* administration of pro-inflammatory cytokines and hydrogen peroxide were alter the various cellular process like dilation & beading of a retinal blood vessel; retinal edema; upregulation of astrogliosis & microglia; and increase the expressions of apoptotic genes

(Huang et al., 2018; Mugisho et al., 2018). Further, visual impairments are altering the retina tissue hyper-excitability; free radical generation, inflammation, calcium accumulation, and a raise in the retinal ganglion cell density. It occurs via the activation of glutamate and N-methyl-D-aspartate (NMDA) receptors (Gómez-Vicente et al., 2015; Tawfik et al., 2021).

The local administration of STZ is potentially caused cellular metabolic abnormalities via the accumulation of free radicals, inflammatory mediators, and neurodegenerative prion proteins (Ashok & Singh, 2018; Pardue & Allen, 2018). The current study results also produced similar bio-molecular changes in retinal tissues *i.e.*, rising in TBARS, and AR activity levels, whereas, it is reduced the level of GSH. It indicates that the direct action of STZ is potentially caused retinal damage and biomarker tissues (Reagan et al., 1999). Besides, visual behaviour changes are also altered *i.e.*, OMR, PM, and TM tests with the local administration of STZ. These changes are significantly correlating with biomarkers and histopathological complications. Experimentally, damage to retinal tissue is proved that it is ameliorated with endogenous molecules like tauroursodeoxycholic acid, and GSH (Gómez-Vicente et al., 2015).

The integrated molecular mechanism in the pathogenesis of DR is too complex. The primary events of DR progression start with the free radical generation, ion channel activation, and enhancement of cellular acidosis environments (Tawfik et al., 2021). The



accumulation of apoptotic proteins, release of cytochrome C, fragmentation of mitochondrial DNA, and expression of various proapoptotic proteins also cause the DR (Kang & Yang, 2020). DEX is a synthetic glucocorticoid and it is widely used in various inflammatory and immunological disorders (Kanda et al., 2020). The DEX and other synthetic glucocorticoids like flucinolone acetonide, and triamcinolone acetonide are widely used and FDA-approved for the treatment of vitreoretinal disorders due to their multitargeted actions (Ryan et al., 2020). Natural medicine *i.e.*, CLS also possesses multitargeted actions like dexamethasone. The multitargeted natural medicines have a promising role in the regulation of the cell signaling process as well as reduction of cellular degradation pathways and repairing of cell damage in various systems of the body (Matteucci et al., 2005; Ojha et al., 2017).

Conclusion

The present study also revealed that CLS is produced the potential ameliorative effects against the STZ-induced DR via potential inhibition of free radical, lipid peroxidation, polyol pathway, neuronal inflammation; and raising of the endogenous antioxidant molecule (GSH). Hence, the hypothesis of our research design has been proved that the administration of CLS ameliorates the DR and it can be used for the management of diabetes-associated secondary complications.

Acknowledgment

Author is thankful to the Faculty of Medicine, AIMST University, 08100 Bedong, Kedah, Malaysia for providing the facilities to conduct this project. The author is also thankful to the Department of Pharmacology, Saveetha Institute of Medical & Technical Sciences (SIMATS), Saveetha University, Chennai-602105, Tamilnadu, India for their continuous support to complete this research work.

Author Contributions: Conceptualization, A.S. and J.T.; Methodology and data analysis, A.S.

and A.M.; Investigation, A.S.; Validation, J.T. and A.M. All authors have read and agreed to the published version of the manuscript.

Funding: None.

Institutional Review Board Statement: The study was conducted according to the guidelines of the AIMST University Animal Ethics committee (protocol approval no: AUAEC/FOM 2020/21 – Amendment No. 1; Dated March 9 November 2020).

Conflicts of Interest: The authors declare no conflicts of interest.

References

- Ashok, A., & Singh, N. (2018). Prion protein modulates glucose homeostasis by altering intracellular iron. *Scientific Reports*, 8(1), 6556. <https://doi.org/10.1038/s41598-018-24786-1>
- Chatziralli, I. (2021). Ranibizumab for the treatment of diabetic retinopathy. *Expert Opinion on Biological Therapy, just-accepted*.
- Deacon, R. M. J., & Rawlins, J. N. P. (2006). T-maze alternation in the rodent. *Nature Protocols*, 1(1), 7.
- Ellman, G. L. (1959). Tissue sulfhydryl groups. *Archives of Biochemistry and Biophysics*, 82(1), 70–77.
- Fouquet, C., Babayan, B. M., Watilliaux, A., Bontempi, B., Tobin, C., & Rondi-Reig, L. (2013). Complementary roles of the hippocampus and the dorsomedial striatum during spatial and sequence-based navigation behavior. *PloS One*, 8(6), e67232.
- Gómez-Vicente, V., Lax, P., Fernández-Sánchez, L., Rondón, N., Esquiva, G., Germain, F., de la Villa, P., & Cuenca, N. (2015). Neuroprotective effect of tauroursodeoxycholic acid on N-methyl-D-aspartate-induced retinal ganglion cell degeneration. *PloS One*, 10(9), e0137826.
- Gora, I. M., Ciechanowska, A., & Ladyzynski, P. (2021). NLRP3 Inflammasome at the Interface of Inflammation, Endothelial Dysfunction, and Type 2 Diabetes. *Cells*, 10(2), 314.
- Guest, P. C. (2019). A Rat Eye Lens Model of



Cataract Formation. In *Pre-Clinical Models* (pp. 311–318). Springer.

Hayman, S., & Kinoshita, J. H. (1965). Isolation and properties of lens aldose reductase. *Journal of Biological Chemistry*, *240*(2), 877–882.

Hong, I. H., Choi, W., & Han, J. R. (2020). The effects of intravitreal triamcinolone acetonide in diabetic macular edema refractory to anti-VEGF treatment. *Japanese Journal of Ophthalmology*, *64*(2), 196–202.

Huang, B., Liang, J.-J., Zhuang, X., Chen, S.-W., Ng, T. K., & Chen, H. (2018). Intravitreal injection of hydrogen peroxide induces acute retinal degeneration, apoptosis, and oxidative stress in mice. *Oxidative Medicine and Cellular Longevity*, *2018*.

Kanda, A., Hirose, I., Yoshida, S., Murata, M., & Ishida, S. (2020). Dexamethasone attenuates hypoxia-and diabetes-induced retinal galectin-1 expression via reducing hypoxia-inducible factor-1 α protein in vitro and in vivo. *Investigative Ophthalmology & Visual Science*, *61*(7), 747.

Kang, Q., & Yang, C. (2020). Oxidative stress and diabetic retinopathy: Molecular mechanisms, pathogenetic role and therapeutic implications. *Redox Biology*, 101799.

Kermorvant-Duchemin, E., Pinel, A. C., Lavalette, S., Lenne, D., Raoul, W., Calippe, B., Behar-Cohen, F., Sahel, J.-A., Guillonneau, X., & Sennlaub, F. (2013). Neonatal hyperglycemia inhibits angiogenesis and induces inflammation and neuronal degeneration in the retina. *PLoS One*, *8*(11), e79545.

Kretschmer, F., Sajgo, S., Kretschmer, V., & Badea, T. C. (2015). A system to measure the Optokinetic and Optomotor response in mice. *Journal of Neuroscience Methods*, *256*, 91–105.

Kuley, B., Storey, P. P., Pancholy, M., Obeid, A., Murphy, J., Goodman, J., Wibbelsman, T. D., Regillo, C., & Chiang, A. (2020). Ocular Hypertension Following Intravitreal Injection of 0.7 mg Dexamethasone Implant versus 2mg Triamcinolone. *Seminars in Ophthalmology*, *35*(2), 141–146.

Lowry, O. H., Rosebrough, N. J., Farr, A. L., & Randall, R. J. (1951). Protein measurement with

the Folin phenol reagent. *J Biol Chem*, *193*, 265–275.

Matteucci, A., Frank, C., Domenici, M. R., Balduzzi, M., Paradisi, S., Carnovale-Scalzo, G., Scoria, G., & Malchiodi-Albedi, F. (2005). Curcumin treatment protects rat retinal neurons against excitotoxicity: effect on N-methyl-D-aspartate-induced intracellular Ca²⁺ increase. *Experimental Brain Research*, *167*(4), 641–648.

Mishra, K. K. (2020). Preservation of Bovine Colostrum: Immunotherapeutic Agents to Promote Health. In *Novel Strategies to Improve Shelf-Life and Quality of Foods* (pp. 3–19). Apple Academic Press.

Mota, R. I., Morgan, S. E., & Bahnson, E. M. (2020). Diabetic vasculopathy: macro and microvascular injury. *Current Pathobiology Reports*, *8*(1), 1–14.

Mugisho, O. O., Rupenthal, I. D., Squirrell, D. M., Bould, S. J., Danesh-Meyer, H. V., Zhang, J., Green, C. R., & Acosta, M. L. (2018). Intravitreal pro-inflammatory cytokines in non-obese diabetic mice: Modelling signs of diabetic retinopathy. *PLoS One*, *13*(8), e0202156.

Nellaippan, K., Kumari, P., Khatri, D. K., & Singh, S. B. (2021). Diabetic Complications: An Update on Pathobiology and Therapeutic Strategies. *Current Diabetes Reviews*.

Ohkawa, H., Ohishi, N., & Yagi, K. (1979). Assay for lipid peroxides in animal tissues by thiobarbituric acid reaction. *Anal Biochem*, *95*, 351–358.

Ojha, S., Balaji, V., Sadek, B., & Rajesh, M. (2017). Beneficial effects of phytochemicals in diabetic retinopathy: experimental and clinical evidence. *Eur Rev Med Pharmacol Sci*, *21*(11), 2769–2783.

Pardue, M. T., & Allen, R. S. (2018). Neuroprotective strategies for retinal disease. *Progress in Retinal and Eye Research*, *65*, 50–76.

Prusky, G. T., Douglas, R. M., Nelson, L., Shabanpoor, A., & Sutherland, R. J. (2004). Visual memory task for rats reveals an essential role for hippocampus and perirhinal cortex. *Proc Natl Acad Sci U S A*, *101*, 5064–5068. <https://doi.org/10.1073/pnas.0308528101> [doi]



0308528101 [pii]

Reagan, L. P., Magarinos, A. M., & McEWEN, B. S. (1999). Neurological changes induced by stress in streptozotocin diabetic rats. *Annals of the New York Academy of Sciences*, 893(1), 126–137.

Robinson, R., Barathi, V. A., Chaurasia, S. S., Wong, T. Y., & Kern, T. S. (2012). Update on animal models of diabetic retinopathy: from molecular approaches to mice and higher mammals. *Disease Models & Mechanisms*, 5(4), 444–456.

Rondi-Reig, L., Petit, G. H., Tobin, C., Tonegawa, S., Mariani, J., & Berthoz, A. (2006). Impaired sequential egocentric and allocentric memories in forebrain-specific-NMDA receptor knock-out mice during a new task dissociating strategies of navigation. *Journal of Neuroscience*, 26(15), 4071–4081.

Ryan, K. M., Boyle, N. T., Harkin, A., & Connor, T. J. (2020). Dexamethasone attenuates inflammatory-mediated suppression of β 2-adrenoceptor expression in rat primary mixed glia. *Journal of Neuroimmunology*, 338, 577082.

Schnichels, S., Paquet-Durand, F., Löscher, M., Tsai, T., Hurst, J., Joachim, S. C., & Klettner, A. (2020). Retina in a dish: Cell cultures, retinal explants and animal models for common diseases of the retina. *Progress in Retinal and Eye Research*, 100880.

Sienkiewicz, M., Szymańska, P., & Fichna, J. (2021). Supplementation of Bovine Colostrum in Inflammatory Bowel Disease: Benefits and Contraindications. *Advances in Nutrition*, 12(2), 533–545.

Tawfik, A., Mohamed, R., Elsherbiny, N. M., DeAngelis, M. M., Bartoli, M., & Al-Shabrawey, M. (2019). Homocysteine: A potential biomarker for diabetic retinopathy. *Journal of Clinical Medicine*, 8(1), 121.

Tawfik, A., Mohamed, R., Kira, D., Alhusban, S., & Al-Shabrawey, M. (2021). N-Methyl-D-aspartate receptor activation, novel mechanism of homocysteine-induced blood–retinal barrier dysfunction. *Journal of Molecular Medicine*, 99(1), 119–130.

Uruakpa, F. O., Ismond, M. A. H., & Akobundu,

E. N. T. (2002). Colostrum and its benefits: a review. *Nutrition Research*, 22(6), 755–767.

Vorhees, C. V., & Williams, M. T. (2014). Assessing spatial learning and memory in rodents. *ILAR Journal*, 55(2), 310–332.

Wang, G., Xie, P., Wang, J., & Min, H. (2020). Retinal Diseases. In *Stereo Atlas of Vitreoretinal Diseases* (pp. 7–110). Springer.

Williams, R., Airey, M., Baxter, H., Forrester, J., Kennedy-Martin, T., & Girach, A. (2004). Epidemiology of diabetic retinopathy and macular oedema: a systematic review. *Eye*, 18(10), 963–983.

Yuan, D., Xu, Y., Hang, H., Liu, X., Chen, X., Xie, P., Yuan, S., Zhang, W., Lin, X., & Liu, Q. (2014). Edaravone protect against retinal damage in streptozotocin-induced diabetic mice. *PLoS One*, 9(6), e99219.

